Available online at www.sciencedirect.com
SCIENCE DIRECT
Catalysis Today 100 (2005) 255–260
CATALYSIS TODAY
www.elsevier.com/locate/cattod

Synthesis, characterization, and unique catalytic performance of the mesoporous material Fe-TUD-1 in Friedel–Crafts benzylation of benzene

M.S. Hamdy [a,b], G. Mul [a], J.C. Jansen [a], A. Ebaid [b], Z. Shan [c], A.R. Overweg [d], Th. Maschmeyer [e,*]

[a] *Delft Chem. Tech., Delft University of Technology, Julianalaan 136, 2628 BL Delft, The Netherlands*
[b] *Chemistry Department, Faculty of Science, Helwan University, Ain Helwan, Cairo, Egypt*
[c] *Technology Development Centre, ABB Lummus Global Inc., Bloomfield, NJ 07003, USA*
[d] *Interfaculty Reactor Institute, Delft University of Technology, Mekelweg 15, 2629 JB Delft, The Netherlands*
[e] *Laboratory of Advanced Catalysis for Sustainability, School of Chemistry, The University of Sydney, Sydney, NSW 2006, Australia*

Available online 23 March 2005

Abstract

Iron (Fe)-containing mesoporous TUD-1 catalysts (denoted as Fe-TUD-1) with different Si/Fe ratios (100, 50, 20 and 10) were synthesized using triethanolamine as a template. They were characterized by XRD, elemental analysis, N_2 ad/desorption measurements, HR-TEM, UV–vis, ^{29}Si NMR, and ^{57}Fe Mössbauer spectroscopies. Catalytic performance was tested in the Friedel–Crafts benzylation of benzene. Fe-TUD-1 showed excellent activity, with 100% conversion and 100% selectivity towards diphenylmethane, superior to other metal-containing TUD-1 (e.g. Ga, Sn, and Ti) or other Fe-containing mesoporous materials (e.g. Fe-MCM-41 and Fe-HMS).

Keywords: Benzylation; Friedel–Crafts; Fe-TUD-1; Mesoporous; Nanoparticles; Benzyl chloride

1. Introduction

Homogeneous acids are commonly used as catalysts in reactions of the Friedel–Crafts type [1]. However, liquid acids, like sulfuric acid, are associated with problems such as corrosion, toxicity, and difficult recovery issues. Therefore, the development of active, solid acid catalysts is an attractive target. For the benzylation of benzene a number of solid catalysts have been reported, such as clays [2,3], polyacid salts [4,5], and zeolites (e.g. HY [6], and H-beta [7]). However, the clays were quite labile even under ambient conditions [8], and polyacids as well as zeolites were not very active [6]. This can often be ascribed to low surface areas (polyacids) or small pore-sizes (zeolites). Mesoporous structures containing accessible and well-dispersed active sites can offer smart alternatives.

The synthesis of Fe-containing mesoporous materials has been reported in the literature as iron can be incorporated as isolated active sites in, e.g. MCM-41 [9,10], MCM-48 [11], and HMS [12], or as nano-particles in various mesoporous systems [13–15]. However, none of the Fe-containing mesoporous materials reported [16,17], although more active than zeolites, did enable complete conversion in the benzylation of benzene over a period of 4 h at 60 °C or of 1.5 h at 75 °C (cf. Table 3). In the case of Fe-MCM-41 the one-dimensional pore structure might introduce a less than optimal diffusion to and from the active centers. For both, Fe-MCM-41 and Fe-HMS, the nature of the active site could also be an issue, since completely isolated Fe-ions may not be the most favourable site. Indeed, nano-sized Fe_2O_3 clusters could prove much more reactive due to their high degree of coordinative unsaturation.

Recently, a new mesoporous silica, TUD-1 [18], with a 3D sponge-like pore structure and high thermal/hydrothermal stability has been synthesized and the variant

* Corresponding author. Tel.: +61 2 9351 2581; fax: +61 2 9351 3329.
E-mail address: th.maschmeyer@chem.usyd.edu.au (T. Maschmeyer).

0920-5861/$ – see front matter © 2004 Elsevier B.V. All rights reserved.
doi:10.1016/j.cattod.2004.10.018

Ti-TUD-1 has been reported [19], in which the template is bi-functional, acting both as a mesopore template and as an complexing agent for titanium ions. At low Ti-loadings, after calcination, accessible, well-dispersed and isolated 4-coordinate titanium centers on the surface of the mesopore walls are obtained, while at high loading mono-dispersed titania (anatase) nanoparticles are formed.

Here, we introduce analogously prepared Fe-TUD-1 and examine its catalytic performance in the Friedel–Crafts benzylation of benzene. In particular, the effects of metal loading have been studied and the material was benchmarked against Fe-MCM-41, Fe-HMS, Fe-ZSM-5 (Fe-MFI) and various metal-TUD-1 materials.

2. Experimental

2.1. Synthesis

Fe-TUD-1 silicas with different Si/Fe ratios have been synthesized according to the molar oxide ratio SiO_2:*x*-Fe_2O_3:0.5TEAOH:1TEA:11H_2O. In a typical synthesis example, i.e. for Fe-1 (for samples nomenclature, cf. Table 1), a mixture of 24 g triethanolamine (97%, ACROS) with 4.5 mL of de-ionized water was added drop-wise into a mixture of 33.2 g tetraethylorthosilicate (+98%, ACROS) and ferric chloride (Aldrich) solution (0.25 g + 5 mL of de-ionized H_2O) while stirring vigorously. After stirring for about 30 min, 32.9 g of tetraethyl ammonium hydroxide (TEAOH, 35%, Aldrich) was added. The mixture was aged at room temperature for 24 h, dried at about 100 °C for 24 h and then hydrothermally treated in a Teflon-lined stainless steel autoclave at 180 °C for 8 h. Finally the solid, as-synthesized samples were calcined at 600 °C for 10 h using a ramp rate of 1 °C/min in air.

2.2. Catalyst characterization

XRD patterns were recorded using Cu Kα radiation (λ = 1541 nm) on a Philips PW 1840 diffractometer equipped with a graphite monochromator. The samples were scanned over the range of 0.1–80° 2θ with steps of 0.02°. *Nitrogen sorption isotherms* were recorded on a Quantachrome Autosorb-6B at 77 K. Mesoporosity was calculated from the adsorption branch using the Barret–Joyner–Halaenda (BJH) model. Diffuse reflectance UV–vis spectra were recorded on a CaryWin 300 spectrometer under atmospheric conditions using $BaSO_4$ as reference. Samples were scanned from 190 to 800 nm. *Elemental analysis* was carried out by using instrumental neutron activation analysis (INAA) [20] on a THER nuclear reactor with a thermal power of 2 MW and maximum neutron reflux of 2.10 m^{-2} s^{-1}. INAA was applied because of difficulties in dissolving the samples. The method proceeds in three steps, irradiation of the elements with neutrons in the nuclear reactor, followed by a period of decay, and finally a measurement of the radioactivity resulting from irradiation. The energy of the radiation and the half-life period of the radioactivity enable a highly accurate quantitative analysis. *^{29}Si MAS NMR* experiments were performed at a magnetic field of 9.4 T on a Varian VXR-400 S spectrometer operating at 104.2 MHz with pulse width of 3.2 ms. Transmission Electron Microscopy (HR-TEM) was carried out on Philips CM30T electron microscope with LaB6 filament as the source of electrons operated at 300 kV. *^{57}Fe Mössbauer* spectra were measured on a constant acceleration spectrometer in a triangular mode with a ^{57}Co:Rh source. Mössbauer spectra were recorded for Fe-5 and Fe-10, both at 300 and 77 K. The overall spectra were deconvoluted with calculated Mössbauer spectra that consisted of Lorentzian-shape lines.

2.3. Catalytic test

The liquid phase Friedel–Crafts benzylation reaction over Fe-TUD-1 was carried out in a magnetically stirred round-bottomed flask fitted with a reflux condenser and heated in a precisely controlled oil bath. The reactions were carried out under N_2 to avoid the effect of moisture. In a typical reaction, 10 mL of benzene (dried over molecular sieves), 0.6 g of 1,2-dichlorobenzene (as internal standard) and 1.0 g of benzyl chloride were added to the catalyst (0.1 g which had been activated overnight at 180 °C). Reaction times and temperatures are given in Table 3. Liquid samples (never more in total than 10% of the reaction volume) were withdrawn at regular intervals and analyzed by gas chromatography on a Varian Star 3500 with a Sil 5 CB capillary column (50 m length, 0.53 mm inner diameter).

Table 1
Elemental analysis, mesoporosity and colors of Fe-TUD-1 samples with different Fe-loadings

Sample	Si/Fe ratio		S_{BET}[a] (m^2/g)	V_{meso}[b] (cm^3/g)	D_{meso}[c] (nm)	Color	
	Synthesis mixture	After calcination				As-synthesized	After calcination
Fe-1	100	113	568	1.82	15.9	Pale yellow	White
Fe-2	50	54	625	1.24	11.5	Pale yellow	White
Fe-5	20	21	803	0.70	5.2	Dark brown	Brownish orange
Fe-10	10	10.1	874	0.45	3.7	Dark brown	Reddish brown

[a] Specific surface area.
[b] Mesopore volume.
[c] Mesopore diameter.

Carrier gas was helium with 5 psi flow pressure. The chromatograph was equipped with a flame ionization detector. Experimental errors were less than 3%.

A leaching experiment was carried out for the Fe-2 sample by separating the solid after 1 h by filtration at reaction temperature, using a micro-membrane filter. The filtrate was quickly returned to the original flask allowing the reaction to proceed further. The solid residue was sent to elemental analysis for quantitative evaluation using the INAA technique.

3. Results and discussion

3.1. Mesoporous structure of Fe-TUD-1

Fig. 1 illustrates XRD patterns of various samples of Fe-TUD-1 as compared with iron oxide (Fe_2O_3) pattern. All Fe-TUD-1 samples showed a single intensive peak at low angle, indicating that Fe-TUD-1 is a meso-structured material. This peak shifted in accordance with the D-spacing of each sample. The peak intensity slightly decreases with the Fe-loading, indicating an influence of Fe loading on the integrity of the mesoporous structure. Additionally no bulk Fe_2O_3 or other phases could be detected in any of the prepared samples.

The elemental analysis and the porosity measurements obtained from N_2 adsorption measurements at 77 K are listed in Table 1. Elemental analysis showed that the Si/Fe ratio obtained after calcination is quite similar to that present in the synthesis gel, which indicates that most of Fe cations are incorporated into the solid final product. All Fe-TUD-1 samples showed type IV adsorption isotherms, indicative for meso-structured character [21]. The pore structure parameters of Fe-TUD-1 showed that the surface area increases with Fe content, while the pore volume and pore diameter decreased.

3.2. Coordination environment of iron

The color of the Fe-TUD-1 samples synthesized is a simple indication for the presence of iron oxide particles [22]. Such particles might not be visible in the powder XRD pattern due to line broadening associated with their small size. The Fe-1 and Fe-2 as-synthesized samples exhibited a pale yellow color (the normal color of as-synthesized TUD-1), suggesting that at that stage no iron oxide was present. However, the as-synthesized Fe-5 and Fe-10 samples were brown. After calcination the Fe-1 and Fe-2 samples were white, the Fe-5 sample was brown/orange while Fe-10 was reddish brown, suggesting the presence of nano-sized extra-framework iron oxide clusters.

The diffuse reflectance UV–vis spectra for the Fe-TUD-1 samples, and for Fe-oxide, are compared in Fig. 2. All Fe-TUD-1 samples exhibit a peak around 260 nm. This band is assigned to the charge transfer between the Fe and O atoms

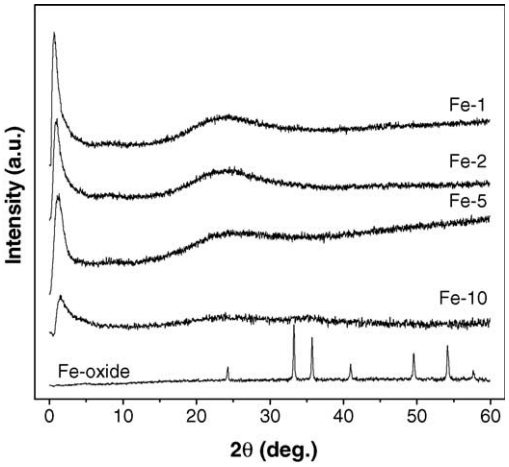

Fig. 1. XRD patterns for Fe-TUD-1.

of Fe–O–Si in the framework, indicating the presence of isolated, tetrahedrally coordinated Fe(III) species [23]. In addition to this peak, a shoulder is apparent at around 330 nm in the Fe-2 sample which would be consistent with the presence of polyferrate $(Fe–O–Fe)_n$ in the framework. At still higher Fe content, for the Fe-5 and Fe-10 samples, two extra peaks are observed around 385 and 518 nm, indicating the presence of either extra-framework iron and/or iron oxide particles with a high Fe-content [24].

3.3. Nano-particles of Fe-oxide inside the TUD-1 matrix

^{29}Si NMR spectra for Si-TUD-1, Fe-1 and Fe-5 are shown in Fig. 3. The chemical shifts with the corresponding peak assignments can be found in the table inset of the figure. The broadening of the peak (−101 ppm) observed in the Fe-1 spectrum may be attributed to the iron incorporation in the silica framework [25–27] of TUD-1, the shift from −101 peak to −99.8 ppm in Fe-5 can be explained by the presence of the strong paramagnetic field of Fe-oxide nano-particles near to the silicon atoms.

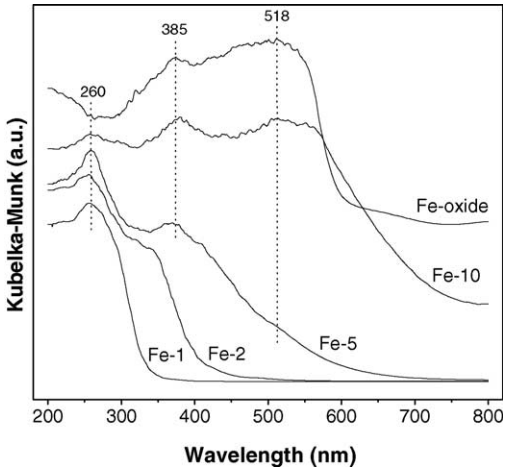

Fig. 2. Diffuse reflectance UV–vis spectra of Fe-TUD-1 samples.

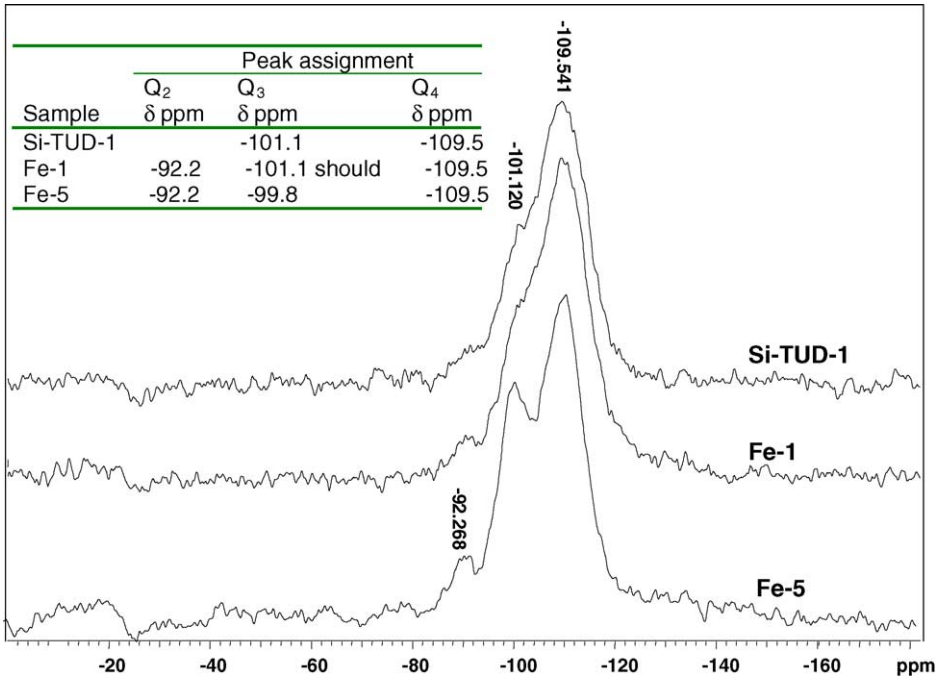

Fig. 3. ^{29}Si MAS NMR spectra for Fe-TUD-1 compared with Si-TUD-1. Inset the chemical shifts observed.

To further illustrate the location of the particles, HR-TEM images were taken of all samples. Fe-1 (Fig. 4a) and Fe-2 images (not presented here) showed only the sponge-like structural characteristic of TUD-1 mesoporous materials, however in the Fe-5 and Fe-10 images (Fig. 4b and c, respectively), the diffraction fringes of embedded iron oxide particles with a size range of 5 and 3 nm for Fe-5 and Fe-10, respectively, can be seen. It is important to note that the mesoporous TUD-1 structure is not visible anymore due to beam damage that occurred while trying to visualize the diffraction fringes of the nanoparticles. Their size range corresponds to that of the Fe-TUD-1 pore diameter, showing an exciting possibility for size-tuning of supported nano-oxide particles.

The ^{57}Fe Mössbauer spectra of Fe-5 and Fe-10 are given in Fig. 5A and B, respectively. The spectral parameters of the fits are summarised in Table 2. The spectra for the two samples consist of a single high-spin Fe(III) component, with spectral parameters that are typical for superparamagnetic Fe-oxide particles. The spectra of both materials recorded at 77 K do not show a transition to a magnetic spectral component implying that the oxide particles are smaller than 4–5 nm in diameter, consistent with the HR-TEM images.

Table 2
Parameters of spectral analysis of ^{57}Fe Mössbauer spectra of Fe-5 and Fe-10 samples

Sample	300 K		77 K	
	Isomer shift (mm/s)	Quadrupole splitting (mm/s)	Isomer shift (mm/s)	Quadrupole splitting (mm/s)
Fe-5	0.60	0.92	0.65	0.96
Fe-10	0.61	0.90	0.70	0.94

3.4. Catalytic activity

In Table 3 the results of the Friedel–Crafts benzylation of benzene over several calcined mesoporous samples are

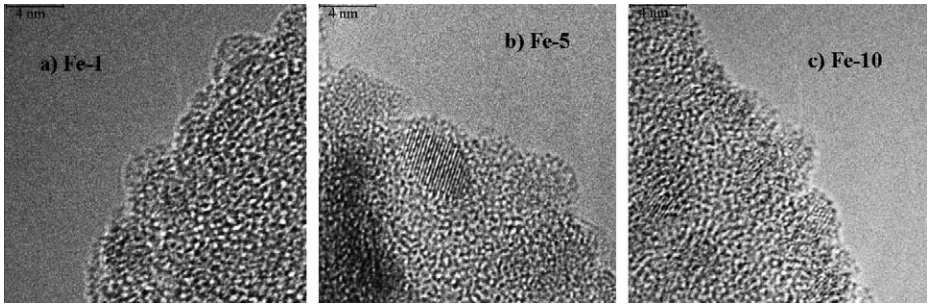

Fig. 4. HR-TEM picture for different Fe-TUD-1 samples.

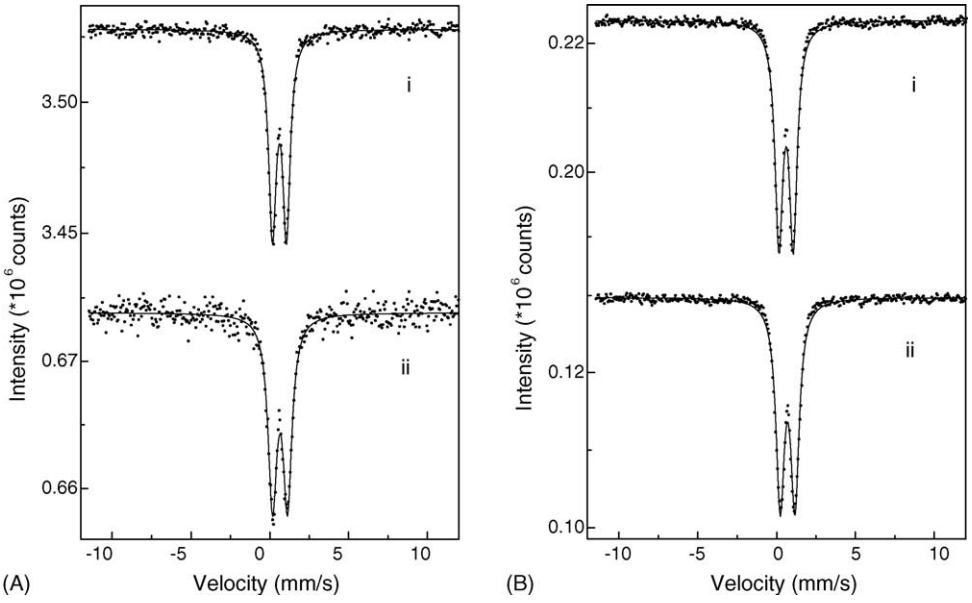

Fig. 5. ^{57}Fe Mössbauer spectra of (A) Fe-5 and (B) Fe-10 at (i) 300 K and (ii) 77 K.

shown. In blank reactions with pure siliceous TUD-1 or with pure Fe_2O_3 powder no product could be found, consistent with the need for iron oxide to be dispersed in TUD-1 to be catalytically active.

For all samples the selectivity to diphenyl methane is 100% (all mass balances are +97%). At 60 °C, Fe-1 converted 86% of benzyl chloride after 4 h; with the Fe-2 sample 100% conversion of benzyl chloride was achieved after 3 h; with the Fe-5 sample 100% conversion was achieved after 10 min, while the Fe-10 achieved 100% conversion within 90 s. This dramatic, non-linear increase of activity as a function of Fe loading points to a change in the nature of the active site.

It is likely that nano-particles of iron oxide will be less coordinatively saturated (due to lattice strain and defects) than isolated iron species, or the iron centers present in larger particles, thereby giving rise to more active centers. The rate of reaction increases with temperature in a proportional way consistent with a reaction of pseudo first order [28].

For the same metal-loading (i.e. Si/M loading = 50), the order of the catalytic activity was Fe-TUD-1 > Ga-TUD-1 > Sn-TUD-1 > Ti-TUD-1, reflecting the standard reduction potential $E^0_{M^{n+}/M}$ of these metals: $E^0_{Fe^{3+}/Fe}$ (−0.037 V) > $E^0_{Ge^{3+}/Ge}$ (−0.560 V) > $E^0_{Sn^{2+}/Sn}$ (−1.375 V) > $E^0_{Ti^{2+}/Ti}$ (−1.630 V) [29]. This is consistent with the idea that redox properties control the reaction and that the mechanism suggested by Choudary et al. [30] holds:

$$Ph{-}CH_2Cl \rightarrow Ph{-}CH_2^{\bullet} + Cl^{\bullet}$$

$$Ph{-}CH_2^{\bullet} + Fe^{3+} \rightarrow Ph{-}CH^{2+} + Fe^{2+}$$

$$Fe^{2+} + Cl^{\bullet} \rightarrow Fe^{3+} + Cl^{-}$$

The filtrate obtained in the leaching experiments is inactive (Fig. 6), although elemental analysis of the residue shows it to contain almost 44% less iron (before reaction the Si/Fe ratio = 54, and after the Si/Fe ratio = 98). Thus, the reaction proceeds over a heterogeneous catalyst represented by category II of Sheldons' leaching classification [31], i.e. the metal is leaching from the solid but does not catalyze the reaction.

Comparing the activity of Fe-TUD-1 with the activities of other mesoporous or even microporous materials, e.g. Fe-MCM-41 [17], Fe-HMS [17,32] and Fe-MFI [33], Fe-TUD-1 is more active. This is most likely due to a combination of an improved local environment of the active site (strained/unsaturated nano-particles), as well as an improved global pore structure in TUD-1. The pore structure might in addition yield a higher accessibility of the 3D framework structure of Fe-TUD-1. More detailed studies on the role of the reducibility of Fe-oxide and the local environment in TUD-1 are in progress.

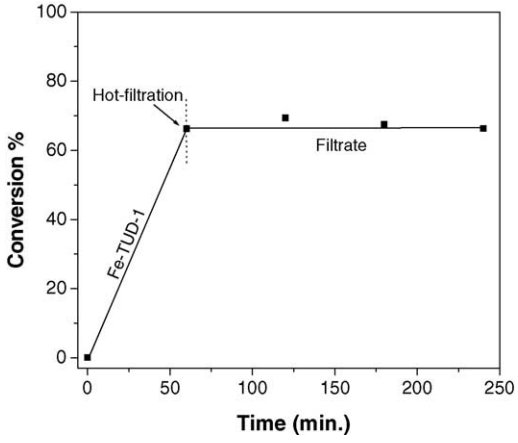

Fig. 6. Conversion of benzyl chloride in catalyst leaching experiment.

Table 3
Comparison between samples compositions and activity (i.e. conversion of benzyl chloride)

Sample	Si/M ratio	Conversion (%)	Reaction time (min)	Temperature (°C)	Reference
TUD-1	∞	0	240	60	Present study
Fe_2O_3	0	0	240	60	Present study
Fe-TUD-1	113	86	240	60	Present study
Fe-TUD-1	54	57	240	40	Present study
Fe-TUD-1	54	100	180	60	Present study
Fe-TUD-1	54	98	30	80	Present study
Fe-TUD-1	21	100	10	60	Present study
Fe-TUD-1	10.1	100	<1.5	60	Present study
Ga-TUD-1	50	65	240	60	Present study
Sn-TUD-1	50	15	240	60	Present study
Ti-TUD-1	50	4.3	240	60	Present study
Fe-HMS	50	73	240	60	17
Fe-MCM-41	62	80	240	60	17
Fe-HMS	23.8	100	120	75	32
Fe-HMS	14	100	90	75	32
Fe-MFI	16.5	90	25	80	33
Fe-AlMFI	28.1	90	104	80	33

4. Conclusions

This study provides a new material, Fe-TUD-1, as a very promising catalyst in Friedel–Crafts' type reactions. Fe-incorporated TUD-1 mesoporous material was synthesized in a one-pot procedure and characterized by several characterization techniques. Fe-TUD-1 exhibits different catalytic sites; at lower Fe-loading only isolated Fe(III) could be detected while at high Fe-loading nano-particles of Fe-oxide embedded inside the mesopores of the TUD-1 silica matrix could be easily identified. Fe-TUD-1 samples showed high activity in benzylation of benzene. The activity increased with Fe-loading, the sample with Si/Fe ratio = 10 being the most active. It was also demonstrated that the reaction is heterogeneously catalyzed and that leaching is not affecting the catalytic results.

Acknowledgements

Dr. P. Kooyman is acknowledged for HR-TEM work, M.S. Hamdy would like to thank the Egyptian government for his personal fellowship. Thanks also to Mr. B. Amer for his experimental assistance.

References

[1] G.A. Olah, Friedel–Crafts and Related Reactions, vol. 1, Wiley/Interscience, New York, 1963 (Chapter 1).
[2] T. Cseri, S. Bekassy, F. Figueras, S. Rizner, J. Mol. Catal. A 98 (1995) 101.
[3] M. Campanati, F. Fazzini, G. Fornasari, A. Tagliani, A. Vaccari, O. Piccolo, Chem. Ind. 75 (1998) 307.
[4] I. Yusuke, O. Mayumi, N. Wataru, U. Kazuo, Chem. Lett. 10 (1992) 1987.
[5] I. Yusuke, O. Mayumi, U. Kazuo, Appl. Catal. A 132 (1995) 127.
[6] B. Coq, V. Gourves, F. Figueras, Appl. Catal. A 100 (1993) 69.
[7] A. Singh, D. Bhattacharya, Catal. Lett. 32 (1995) 327.
[8] E. Rightor, M. Tzou, T. Pinnavaia, J. Catal. 130 (1991) 29.
[9] Z.Y. Yuan, S.Q. Liu, T.H. Chen, J.Z. Wang, H.X. Li, J. Chem. Soc., Chem. Commun. 9 (1995) 973.
[10] B. Echchahed, A.R. Badiei, F. Beland, L. Bonneviot, Stud. Surf. Sci. Catal. 117 (1998) 559.
[11] W. Zhao, Y. Luo, P. Deng, Q. Li, Catal. Lett. 73 (2001) 199.
[12] N.Y. He, J.M. Cao, S.L. Bao, Q.H. Xu, Mater. Lett. 31 (1997) 133.
[13] M. Iwamoto, T. Abe, Y. Tachibana, J. Mol. Catal. A 155 (2000) 143.
[14] P. Selvam, S.E. Dapurkar, S.K. Badamali, M. Murugasan, H. Kuwano, Catal. Today 68 (2001) 69.
[15] R. Kohn, M. Froba, Catal. Today 68 (2001) 227.
[16] N. He, S. Bao, Q. Xu, Appl. Catal. A 169 (1998) 29.
[17] J. Cao, N. He, C. Li, J. Dong, Q. Xu, Stud. Surf. Sci. Catal. 117 (1998) 461.
[18] J.C. Jansen, Z. Shan, L. Marchese, W. Zhou, N. Puil, T. Maschmeyer, Chem. Commun. (2001) 713.
[19] Z. Shan, E. Gianotti, J.C. Jansen, J.A. Peters, L. Marchese, T. Maschmeyer, Chem. Eur. J. 7 (2001) 1437.
[20] F. Boynton, Neutron activation analysis, in: K. Gschneidner, Jr., L. Eyring (Eds.), Handbook on the Physics and Chemistry, vol. 4, North-Holland Publishing Company, Amsterdam, 1979, pp. 457–470(Chapter 37F).
[21] K. Sing, D. Everett, R. Haul, L. Moscou, R. Pierotti, J. Rouquerol, T. Siemieniewska, Pure Appl. Chem. 57 (1985) 603.
[22] P. Ratnasami, R. Kumar, Catal. Today 9 (1991) 329.
[23] B. Echchahed, A. Moen, D. Nicholson, L. Bonneviot, Chem. Mater. 9 (1997) 1716.
[24] Y. Wang, Q. Zhang, T. Shishido, K. Takehira, J. Catal. 209 (2002) 186.
[25] W.A. Carvalho, P.B. Varaldo, M. Wallau, U. Schuchardt, Zeolites 18 (1997) 408.
[26] M. Alves, H. Pastore, Micropor. Mesopor. Mater. 47 (2001) 397.
[27] S. Bruni, F. Cariati, M. Casu, A. Lai, A. Musimu, G. Piccaluga, S. Solinas, NanoStruct. Mater. 11 (1999) 573.
[28] V.R. Choudhary, S.J. Jana, Appl. Catal. A 224 (2002) 51.
[29] R. Weast, M. Astle, W. Beyer, Handbook of Chemistry and Physics, 64th ed., 1985.
[30] B.M. Choudary, M.L. Kantam, M. Sateesh, K.K. Rao, P.L. Santhi, Appl. Catal. A 149 (1997) 257.
[31] I.W.C.E. Arends, R.A. Sheldon, Appl. Catal. A 212 (2001) 175.
[32] K. Bachari, J.M.M. Millet, B. Benaichouba, O. Cherifi, F. Figueras, J. Catal. 221 (2004) 55.
[33] V.R. Choudhary, S.K. Jana, B.P. Kiran, Catal. Today 59 (1999) 217.